Available online at www.sciencedirect.com

SCIENCE DIRECT®

Thin Solid Films 468 (2004) 120–124

www.elsevier.com/locate/tsf

# Influences of current density on structure and corrosion resistance of ceramic coatings on Ti–6Al–4V alloy by micro-plasma oxidation

Zhongping Yao*, Zhaohua Jiang, Xuetong Sun, Shigang Xin, Yanping Li

*Department of Applied Chemistry, Harbin Institute of Technology, No. 92 Xidazhijie Street, Nangang District, Harbin 150001, PR China*

Received 14 August 2003; received in revised form 30 March 2004; accepted 13 May 2004
Available online 24 June 2004

**Abstract**

Current density is a key factor during micro-plasma oxidation (MPO) process. Its influences on structure, morphology and corrosion resistance of ceramic coatings on Ti–6Al–4V by pulsed bi-polar micro-plasma oxidation in $NaAlO_2$ solution were studied in this paper. The ceramic coatings are composed of $Al_2TiO_5$, $\alpha$-$Al_2O_3$ and rutile $TiO_2$, of which $Al_2TiO_5$ is the main crystalline. Compared with the condition of the same current density for both pulses, the rise of cathode current density led to an increase in the amount of rutile $TiO_2$, decreased the thickness and made the coatings compact; whereas the rise of anode current density led to an increase in the amount of $\alpha$-$Al_2O_3$, increased the thickness and made the coatings coarse and porous. Whether increasing anode current density or cathode current density, there were more micro-holes on the surface of the coatings than that of same current density for both pulses. Besides, the corrosion resistance properties of the coated samples were better than that of Ti–6Al–4V substrate, whether considering the point corrosion resistance or the general corrosion resistance. When the anode current density ($I_a$) and the cathode current density ($I_c$) were both equal to 8 A/dm$^2$ ($I_a/I_c$ = 8/8 A/dm$^2$), or $I_a$ = 8 A/dm$^2$ and $I_c$ = 10 A/dm$^2$ ($I_a/I_c$ = 8/10 A/dm$^2$), the produced coatings had the best point corrosion resistance, and the latter was a little better than the former. When $I_a/I_c$ = 10/8 A/dm$^2$, the produced coating's general corrosion resistance was best.


*Keywords:* Micro-plasma oxidation; Ceramic coatings; Corrosion; Titanium alloy

## 1. Introduction

The micro-plasma oxidation (MPO) technique, by which a compound ceramic coating is grown in situ on Al, Ti, Mg and many other valve-metals directly, has been developed rapidly in recent years [1–6]. This technique is easy operating, has high efficiency, low pollution, and is convenient for adjusting of technique parameters and adding of other substances into electrolyte, which can easily change the microstructure of the coatings. Coatings produced by the MPO tech. have both fine properties of ceramic coatings and good cohesion between Ti–6Al–4V substrate and the coating, which, therefore, has a wide promising prospect of the application [7–9]. Current density is a key factor of the MPO technique, which influences all sorts of characters of ceramic coatings. At present, there are only a few instances of research work with the MPO technique on Al alloy with current density [10,11], such work on Ti and its alloy is seldom reported [12–14]. Besides, among Ti and its alloys, Ti–6Al–4V alloy is the most widely used in many fields all over the world. Therefore, we prepared the compound ceramic coatings on Ti–6Al–4V alloy by pulsed bi-polar micro-plasma oxidation in $NaAlO_2$ solution, and discussed the influences of current density of both pulses on phase composition, structure and corrosion resistance of the ceramic coatings.

## 2. Experimental details

### 2.1. Preparing of compound ceramic coatings by micro-plasma oxidation technique

Disc samples of Ti–6Al–4V with a diameter of 16 mm and thickness of 6 mm were first polished with abrasive

* Corresponding author. Tel.: +86-451-86413710; fax: +86-451-86413709.
*E-mail address:* yaozhongping@hit.edu.cn (Z. Yao).

0040-6090/$ - see front matter © 2004 Elsevier B.V. All rights reserved.
doi:10.1016/j.tsf.2004.05.075

paper, and then washed in $HF-HNO_3$ (1:1 in volume) aqueous solution. A home-made high power pulsed bipolar electrical source with power of 5 kW was used for micro-plasma oxidation of the disc samples in a water-cooled electrolyser made of stainless steel, which also serves as the counter electrode. The reaction temperature was controlled to below 30 °C by adjusting the cooling water flow. The MPO process equipment used is similar to the one presented by Matthews' group in Ref. [1]. The electrical source frequency was fixed at 60 Hz. The concentration of $Na_2AlO_2$ used in the experiment was 8 g/l and that of $Na_3PO_4$ 1 g/l. The whole process was divided into two stages: (1) a constant current density period when the constant current density was applied to the sample for 60 min, then (2) a current-descending period when current density was allowed to decrease freely until the whole reaction time reached 90 min. After the treatment, the excess of electrolyte solution on the coated samples was rinsed with water and the samples dried in the air. Three samples were made under each conditions of current density to ensure the reliability of the experiments.

### 2.2. Analysis of phase composition and structure of the coatings

Phase composition of the coatings was examined with X-ray diffraction (XRD), with a Cu Kα source. Morphology images of the prepared coatings were studied with scanning electron microscopy (SEM) (Japan Hitachi S-570). Sample thickness was measured, using an eddy current based thickness gauge (CTG-10, Time), which minimum resolution is 1 μm with an accuracy of 0.1 μm. In this experiment, the average thickness of each of the triplicate samples was obtained from 10 measurements at different positions.

### 2.3. Evaluation of corrosion resistance properties of the coatings

Accelerated electrochemical method in a three-electrode cell (Pt plate was used as counter electrode, Ag/AgCl electrode auxiliary electrode, the coated sample working electrode) through CHI1140 electrochemical analyzer (Shanghai, China) was used to assess the corrosion resistance properties of the coated samples in aerated 3.5% NaCl solution. Point corrosion resistance was evaluated by potentiodynamic anodic scanning curves. The potentiodynamic scanning rate was 20 mV/s, with a potential raise from 0 to 7 V, returning to 0 V, forming a potential–current density curve. General corrosion resistance of the coating was evaluated by polarizing curves. The polarization curve scanning rate was 10 mV/s, with a scanning range from −0.25 V of open circuit potential to +0.25 V of open circuit potential.

## 3. Results and discussion

### 3.1. Influences of electronic current density on morphology and composition of the coatings

Current density affects the coatings' thickness, appearance and many other features. Under the condition of the same current densities for both pulses, the produced coatings were of different thickness and appearance: the coatings produced at less than 6 A/dm$^2$ were uniform and less than 50 μm; while the ones obtained at more than 10 A/dm$^2$ were coarse, porous and more than 100 μm, and especially, had the poor adhesion to the substrate. Generally, when prepared using 6-10 A/dm$^2$, the obtained coatings were dense, uniform and adhered well to the substrate, with the thickness of between 50 and 100 μm in our experiments. However, under different anode and cathode current densities, the produced coatings also had different features. When the anode current density ($I_a$) and the cathode current density ($I_c$) were both equal to 8 A/dm$^2$, the coatings were compact and the color was a little grayish yellow. If the anode current density was increased, the coatings turned grayer, more porous and less compact. If the cathode current density was increased, the coatings turned yellow and looked more compact. The thickness of the coatings under different current densities is shown in Table 1.

Further studies on the morphology of the coatings were made by SEM analysis of the coatings, which is shown in Fig. 1. Panels (a) and (d) are the surface and cross-section images of the coatings of $I_a/I_c = 8/10$ A/dm$^2$, respectively; panels (b) and (e) the surface and cross-section images of the coatings of $I_a/I_c = 8/8$ A/dm$^2$, respectively; and panels (c) and (f) the surface and cross-section images of the coatings of $I_a/I_c = 10/8$ A/dm$^2$, respectively. It is to be noted that the coatings of panels (a) and (c) had more pores than that of panel (b), and the pores of (a) were bigger than that of (c), which may be related with the non-symmetry of both current densities. In the same way, the coating of panel (d) was more compact and thinner than that of panel (e), whereas the coating of panel (f) was coarser than that of panel (e), but had the similar thickness with that of panel (e). According to the explanation given by Yerokhin et al. [2], the effect of negative half-cycles is that it probably leads to the dissolution of some oxide phase on the coating surface. Therefore, the rise of the cathode current density resulted in the dissolution of more oxide phase, which was certain to decrease the thickness of the coatings, meantime the coat-

Table 1
Thickness of the coatings under different anode and cathode current densities

| $I_a/I_c$ (A/dm$^2$) | 8/10 | 8/8 | 10/8 |
|---|---|---|---|
| Mean thickness (μm) | 76.1 | 89.7 | 109 |
| Max thickness (μm) | 83 | 97 | 124 |
| Min thickness (μm) | 69 | 83 | 90 |
| Standard deviation | 4.7 | 4.1 | 5.6 |

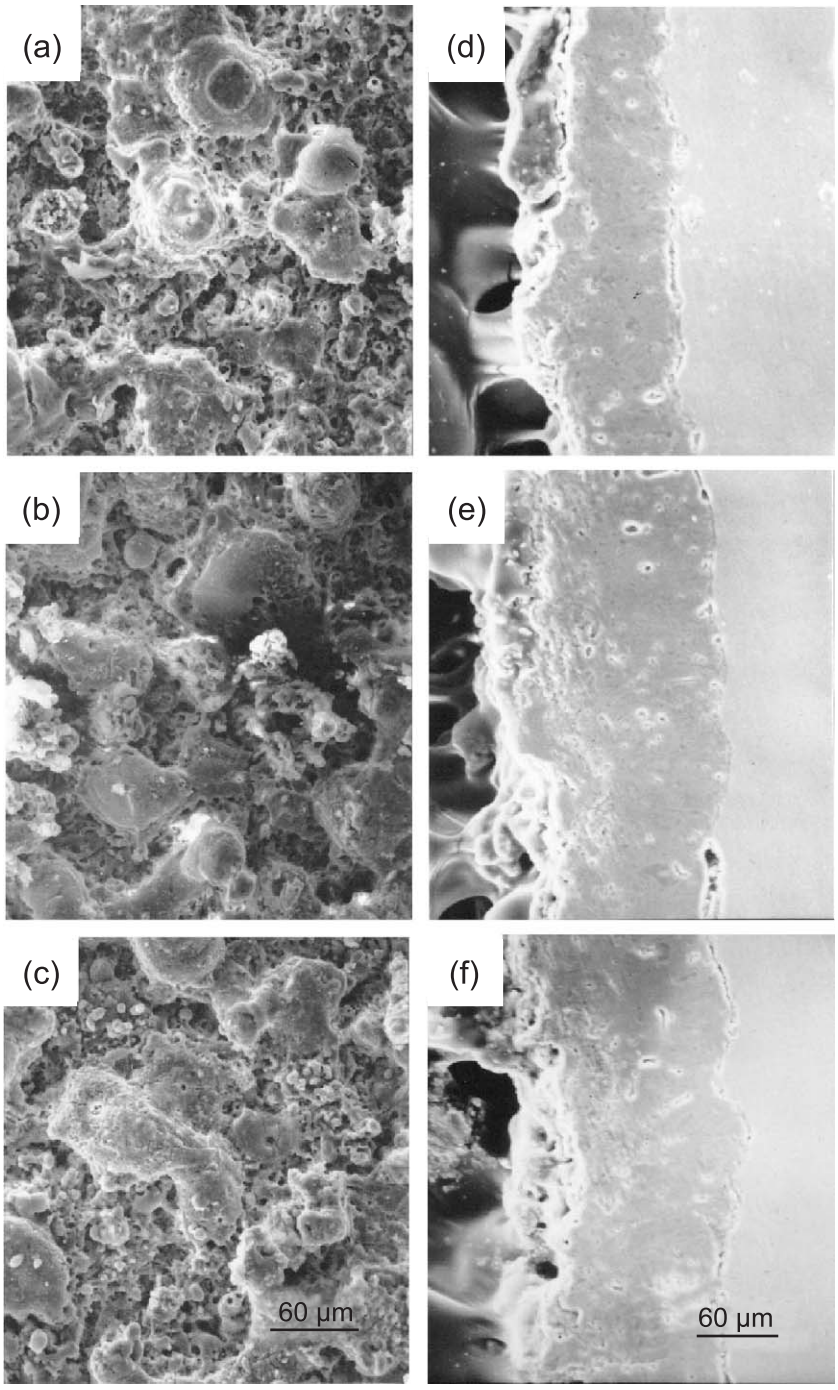


Fig. 1. SEM morphology of surface ((a), (b), (c)) and section ((d), (e), (f)) of the coatings of different current densities. (a and d) $I_a/I_c = 8/10$ A/dm$^2$; (b and e) $I_a/I_c = 8/8$ A/dm$^2$; (c and f) $I_a/I_c = 10/8$ A/dm$^2$.

ings turned more compact and less porous, as seen in panel (d). Similarly, when the anode current density was increased, which also meant the effect of cathode current density was weakened comparatively, in this way the coatings turned more porous and less compact, as seen in panel (f), and the thickness of the coatings was also increased, as seen in Table 1. However, the thickness of the coatings in panel (f) clearly is not consistent with that in Table 1, which is because the surface of the coatings was so loose and coarse that it was easily embedded or destroyed by resin.

The differences of the coatings under different anode and cathode current densities are also related with their phase composition. The influence of current density on phase composition of the ceramic coatings is shown in Fig. 2. It is clearly shown from Fig. 2 that the coatings are composed of a large amount of $Al_2TiO_5$ and $\alpha$-$Al_2O_3$, as well as a

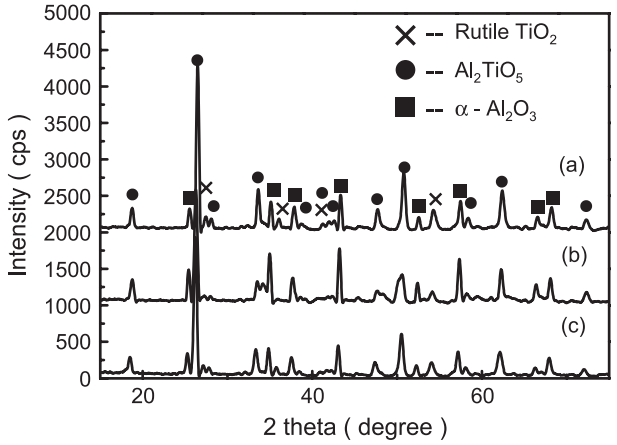


Fig. 2. XRD patterns of the coatings of different anode and cathode current densities. (a) $I_a/I_c = 8/8$ A/dm$^2$; (b) $I_a/I_c = 10/8$ A/dm$^2$; (c) $I_a/I_c = 8/10$ A/dm$^2$.

small amount of rutile $TiO_2$. The amount of α-$Al_2O_3$ and rutile $TiO_2$ varied according to the changing of the anode and cathode current density. If the anode current density was increased, the amount of α-$Al_2O_3$ of the coatings increased greatly; if the cathode current density was increased, the amount of α-$Al_2O_3$ decreased a little comparatively. As to rutile $TiO_2$, the changing trend was quite opposite: the rise of the cathode current density led to an increase in the amount of rutile $TiO_2$, while the rise of the anode current density led to a decrease in the amount of rutile $TiO_2$.

### 3.2. Corrosive resistant properties of ceramic coatings

#### 3.2.1. Point corrosion resistance of the ceramic coatings

Current density has influenced the phase composition and morphology of the coatings, and therefore, it is bound to influence the corrosion resistance of the coatings. The potentiodynamic anodic scanning curves of the coated samples and Ti–6Al–4V substrate are shown in Fig. 3. Fig. 3(b) is the enlarged picture of part of Fig. 3(a). In terms of the scanning curves, it is easily found that the point corrosion took place for the substrate and the coatings of $I_a/I_c = 10/8$ A/dm$^2$, and there was no point corrosion for the coatings of $I_a/I_c = 8/8$ A/dm$^2$ and $I_a/I_c = 8/10$ A/dm$^2$. The area of the closed curves of the coatings of $I_a/I_c = 8/10$ A/dm$^2$ was smaller than that of the substrate, and its current density was also lower than that of the substrate, so the point corrosion resistance of the coating of $I_a/I_c = 10/8$ A/dm$^2$ was better than that of the substrate. In addition, the coating of $I_a/I_c = 8/10$ A/dm$^2$ was a little better than that of $I_a/I_c = 8/8$ A/dm$^2$ because the current density of the former was almost always lower than that of the latter as the increased scanning potential. In short, the point corrosion resistance of the coated samples was obviously much better than that of Ti–6Al–4V substrate; and among the coated samples, the best coatings were the ones of $I_a/I_c = 8/10$ A/dm$^2$ and $I_a/I_c = 8/8$ A/dm$^2$, they were much better than that of $I_a/I_c = 10/8$ A/dm$^2$, which shows that the key factors for the point

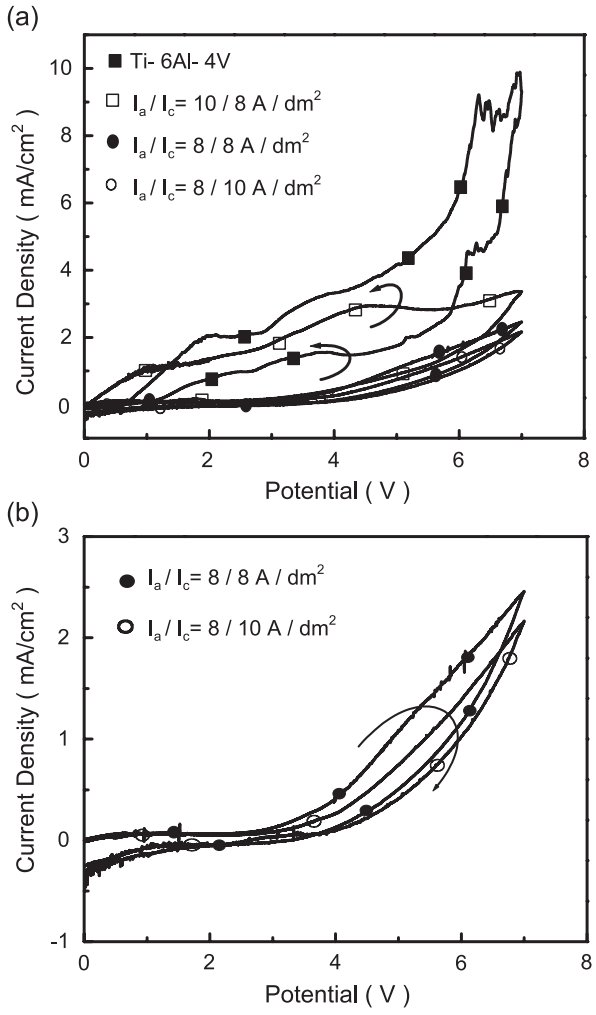


Fig. 3. Potentiodynamic anodic curves of the coated samples of different current densities and Ti–6Al–4V substrate in aerated 3.5% NaCl solution. (b) is the enlarged picture of part of (a).

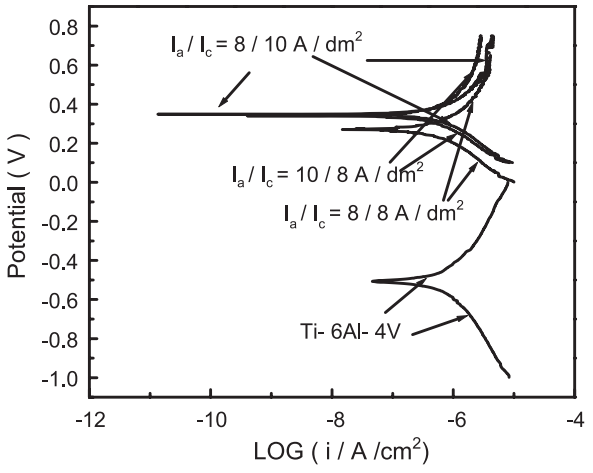


Fig. 4. Polarization curves of the coated samples of different current densities and Ti–6Al–4V substrate in aerated 3.5% NaCl solution.

Table 2
Corrosion current density and corrosion potential of Ti–6Al–4V substrate and the coated samples under different current densities

| $I_a/I_c$ (A/dm$^2$) | Corrosion current density (A/cm$^2$) | Corrosion potential (V) |
|---|---|---|
| Ti–6Al–4V | $9.980 \times 10^{-7}$ | −0.507 |
| 8/8 | $7.234 \times 10^{-7}$ | 0.270 |
| 8/10 | $7.454 \times 10^{-7}$ | 0.348 |
| 10/8 | $5.222 \times 10^{-7}$ | 0.340 |

corrosion resistance may be the compactness, low porosity, and the content of rutile $TiO_2$ in the coatings, not the thickness of the coatings. The proper increase of the cathode current density increased the amount of the rutile $TiO_2$ in the coatings, and made the coating more and more compact, and therefore, the point corrosion resistance of the coatings was improved.

*3.2.2. General corrosion resistance of the coatings*

Since the variation of current density has affected the point corrosion resistance of the coatings greatly, another study was made to evaluate the general corrosion resistance of the coatings by polarizing curve test. Polarizing curves of the coated samples and Ti–6Al–4V substrate are shown in Fig. 4, and the corrosion current density and the corrosion potential of the coated samples and Ti–6Al–4V substrate are seen in Table 2. Corrosion current densities of the coated samples were all a little lower than that of Ti–6Al–4V substrate and the corrosion potentials all moved to the higher in comparison with that of Ti–6Al–4V substrate. Therefore, the general corrosion resistance of the coated samples was improved to certain extent. But among the coated samples under different conditions, the best one was the coating of $I_a/I_c = 10/8$ A/dm$^2$, its corrosion current density was of the minimum. Also, the corrosion current densities of the coatings under the other two conditions were similar. This illustrates that the thickness of the coatings may be the most important factor for the general corrosion resistance, and the proper increase of anode current density is helpful for the improvement of the general corrosion resistance of the coatings.

## 4. Conclusion

The current density of anode and cathode pulse has influenced the phase composition, morphology and corrosion resistance of the coatings, as a key technique parameter during the MPO process. The produced coatings on Ti–6Al–4V by micro-plasma oxidation in $NaAlO_2$ solution are composed of $Al_2TiO_5$, $\alpha$-$Al_2O_3$ and rutile $TiO_2$. Compared with the condition of the same current density for both pulses, the rise of cathode current density led to an increase in the amount of rutile $TiO_2$ in the coatings, and decreased the thickness and made the coatings compact; whereas the rise of anode current density led to an increase in the amount of $\alpha$-$Al_2O_3$ in it, and increased the thickness and made the coatings coarse and porous. The corrosion resistance of the coated samples was better than that of Ti–6Al–4V substrate, whether considering the point corrosion resistance or the general corrosion resistance. The proper increase of cathode current density is helpful for the improvement of the point corrosion resistance of the coatings, whereas the proper increase of the anode current density is helpful for the improvement of the general corrosion resistance.

## Acknowledgements

This work was financially supported by National Natural Science Foundation of China (Grant No. 50171026).

## References

[1] A.L. Yerokhin, X. Nie, A. Leyland, A. Matthews, S.J. Dowey, Surf. Coat. Technol. 122 (1999) 73.
[2] A.L. Yerokhin, X. Nie, A. Leyland, A. Matthews, Surf. Coat. Technol. 130 (2000) 195.
[3] P.I. Butygin, Ye.V. Khokhryakov, A.L. Mamaev, Mater. Lett. 57 (2003) 1784.
[4] B.L. Jiang, S.F. Zhang, G.J. Wu, T.Q. Lei, Chin. J. Nonferr. Met. 12 (2002) 454 (in Chinese).
[5] Z.H. Jiang, S.G. Xin, F.P. Wang, Chin. J. Nonferr. Met. 10 (2000) 519 (in Chinese).
[6] Z.L. Tang, F.H. Wang, W.T. Wu, P.S. Gordienko, S.V. Gnedenkov, V.S. Rudnev, Chin. J. Nonferr. Met. 9 (1999) 63 (in Chinese).
[7] X. Nie, E.I. Meletis, J.C. Jiang, A. Leyland, A.L. Yerokhin, A. Matthews, Surf. Coat. Technol. 149 (2002) 245.
[8] W.B. Xue, C. Wang, Y.L. Li, Z.W. Deng, R.Y. Chen, T.H. Zhang, Mater. Lett. 56 (2002) 737.
[9] X.H. Wu, Z.H. Jiang, F.P. Wang, S.G. Xin, H.Q. Ben, Chin. J. Nonferr. Met. 11 (2001) 806 (in Chinese).
[10] G. Sundrarajan, L. Rama Krishna, Surf. Coat. Technol. 167 (2003) 269.
[11] G.L. Yang, X.Y. Lv, Y.Z. Bai, H.F. Cui, Z.S. Jin, J. Alloys Compd. 345 (2002) 196.
[12] A.L. Yerokhin, A. Leyland, A. Matthews, Appl. Surf. Sci. 200 (2002) 172.
[13] C.T. Wu, F.H. Lu, Surf. Coat. Technol. 166 (2003) 31.
[14] W.B. Xue, C. Wang, Z.W. Deng, R.Y. Chen, T.H. Zhang, Mater. Sci. Technol. 18 (2002) 37.